Acta Polytechnica **64**(1):42–51, 2024
https://doi.org/10.14311/AP.2024.64.0042

Published by the Czech Technical University in Prague

OUTDOOR PERFORMANCE INVESTIGATION OF A THERMOELECTRIC COOLER-INTEGRATED SOLAR AIR HEATING COLLECTOR

Josué R. Segnon*, Howard O. Njoku

University of Nigeria, Sustainable Energy Engineering Research Group, Department of Mechanical Engineering, 410001 Nsukka, Nigeria

* corresponding author: josue.segnon.pg90595@unn.edu.ng

Abstract. Solar air heating systems are continuously being improved by combining them with other energy conversion technologies. In this paper, outdoor tests were carried out on a thermoelectric heat-pumping solar air heater (TE-SAH), with four (04) TECs (TEC1–12706) attached to the backside of the absorber plate, and powered by a 40 Wp mono-Si PV module to pump heat from the absorber plate into the heated air. The thermal energy production, energy efficiency, heat loss coefficients, and heat removal factor were evaluated and compared with a reference system without TECs. The heat collection and energy efficiency of the solar air heater were improved by 7.14 % and 66.71 %, respectively, with the integration of TECs. Heat losses also decreased by 0.46 MJ. Furthermore, the estimated heat removal factor for the TE-SAH was 0.55, higher than 0.49 obtained for the reference SAH. These results showed that PV-TE heat-pumping is a viable means of improving the thermal performance of solar air heaters.

Keywords: Solar air heating, thermoelectric cooler, heat pumping, heat collection, energy efficiency.

1. Introduction

Renewable energy is at the forefront of the ongoing transition towards a cleaner and sustainable energy supply. Among the renewable energy sources, solar energy is the most preferred option for use globally due to the relatively low maintenance costs of associated technologies [1]. Solar radiation can also be converted into useful heat by use of solar heating systems for application in cooling, heating, crop drying, ventilation, cooking, etc. [2, 3]. In solar heating systems, water, air, nanofluids, or any combination can be used as the working fluid. In solar air heating systems, the solar air heater (SAH) captures the solar radiation on a blackened surface (absorber plate), thus heating the plate, and transferring this heat to the working air that absorbs useful heat as it flows past the plate. Systems that combine solar technologies with other energy conversion technologies have considerably increased energy outputs compared to the standalone solar energy conversion technologies [4, 5]. For instance, photovoltaic-thermal (PVT) systems produce both thermal and electrical energies from the same absorbing surface and achieve higher energy conversion efficiencies than standalone PV or solar thermal systems [6, 7]. Also, thermoelectric modules (TEMs), when coupled with PV modules, produce additional electrical power, hence achieving a higher output than both the standalone PV and TEMs.

Thermoelectric generators (TEGs) are semiconductor devices that directly convert a temperature difference into electricity, based on the Seebeck effect. This concept has been presented as a means of improving the electrical energy output by attaching the TEGs at the back of PV modules, thus converting the temperature difference between the PV module and the adjacent air into additional electricity, as shown in Figure 1 [5]. Thus, with the same PV absorbing surface, this combination could improve the system power output by up to 15 % [8–11]. The same principle is applied in PVTs, increasing the overall efficiency of the module [12–14]. However, this combination only converts the temperature difference into electricity without any focus on the thermal output of the system. The heat is not removed from beneath the absorbing surface, negatively affecting the performance of the system.

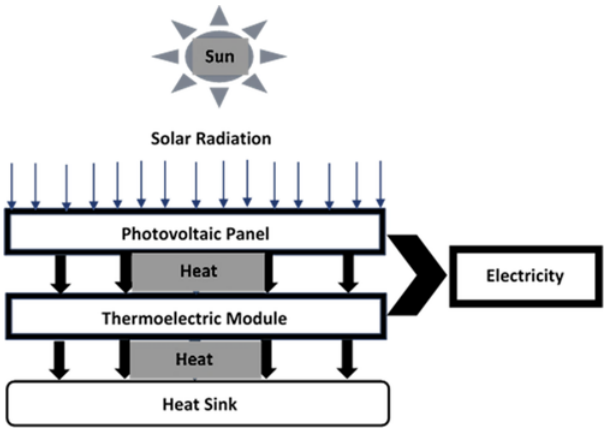

Figure 1. Schematic of an integrated solar PV-TEG system [8].

Based on the Peltier effect, TE modules (TE cool-

ers in this case), can perform either heating or cooling when powered with electricity produced by e.g. PV modules (Figure 2). This offers the features of compactness, easy mobility, and environmental-friendliness in surface cooling [15–17]. Luo et al. [18] numerically compared the performance of a building-integrated PV wall (BIPV) and a building-integrated PV-TE wall (BIPVTE) to that of a massive wall. Compared to the massive wall, the energy saving ratio of the BIPVTE was reported to be up to 172 % higher, while that for the BIPV was just 40 % higher. Wang et al. [19] also reported a BIPVTE system that could achieve an annual CO_2 emission reduction of 4305.4 kg/year. TE coolers have been used to pump heat from a PV module to lower its temperature by 18 °C and improve the electrical output of the system by 2–3 % [20, 21]. Thus, applying the TE cooling could also improve the performance of solar energy conversion systems.

Solar-TE systems have also been widely applied in water desalination, cold storage, refrigeration, and air conditioning, etc. [22–24]. Allouhi et al. [25] reported that space heating using PV-TE integrated walls with 12 TE modules heated a $3 \times 3 \times 2.8$ m room from 24 °C to 37.8 °C. The system achieved a maximum COP of 2.0 and an annual energy saving 64.0 % higher than the conventional electric heating system. Cai et al. [26] modelled the air cooling and water production using TE heat pumping and reported that by increasing the input power to the TE modules, the total cooling load increased but the system efficiency decreased significantly.

In solar air heaters, the system performance largely depends on the effectiveness of the heat extraction from the absorber plate. The existing methods for increasing heat extraction include the use of fins, baffles, porous absorbers, multiple pass designs, and an increase in the airflow rate. With these methods, SAH energy efficiencies have been improved by up to 61 % [27–29]. SAHs can also be combined with PV modules to form a PVT collector which provides both electricity and heat. In addition to the heat produced by the PVT's thermal collector, heat is removed from the PV module as well, cooling it, and thus improving both thermal and electrical energy outputs. Early PVT designs used fluid coolants, air, and later liquids, such as water and glycols, as heat exchange fluids. Other considerations have led to the use of PCMs, nano-fluids, heat pipes, micro-scale heat exchangers, and thermoelectric modules [30, 31]. The combined energy efficiency (electrical and thermal) of such hybrid systems ranges from 31 % to 94 %, as reported by Diwania et al. [4] and Oner et al. [32].

Although TE heat pumping has been shown to improve the performance of heating/cooling systems, the existing literature for solar-TE cooling has focused on improving the electrical performance of PV modules, and no work, to date, extensively studied TE heat extraction from SAH's absorber plate. In this paper, a

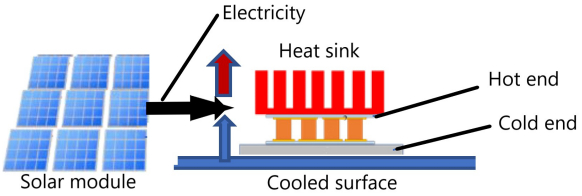

FIGURE 2. Schematic of a solar-powered TE cooling system [33].

novel approach to improving the thermal performance of SAHs using TE heat pumping has been investigated experimentally. The solar irradiance incident on the collector is converted into both heat and electricity by its absorber and a PV module, respectively. The electricity produced by the PV module is used to power TECs with their cold side attached to the absorber plate. These TECs then pump heat from the absorber plate and transfer it to the adjacent air flowing through the collector. The heat is then released at the hot end and dissipated into the working air flowing through the collector. Hence, the heat collection is improved. The absorber plate is cooled by the TEC heat pumping, lowering the temperature gradient between the absorber plate and the ambient, thus reducing heat losses to the ambient. This results in a better performance of the system. The energy flow diagram of the proposed system is presented in Figure 3. The input of the system is solar radiation, and the output is the thermal energy, improved by the PV-powered TE heat pumping. Figure 4 shows a graphical comparison of a TE heat pumping (HP) solar air heater and a conventional SAH. In the conventional SAH, elevated absorber temperatures cause significant heat losses to the atmosphere. In the TE-HP-SAH, TECs are powered by the PV module to pump heat from the absorber plate. The heat is then dissipated into the air channel to reduce the absorber temperatures and lower heat losses to the atmosphere. Thus, the heat gain of the air is increased.

2. Materials and methods

2.1. System description

The solar air heater construction consisted of a glazed wooden casing with 25 mm insulation on its sides and bottom to reduce conduction losses to the ambient. The space beneath the absorber plate served as a channel for airflow through the collector. A 40 Wp mono-Si PV module was placed adjacent to the thermal collector. The overview of the system is shown in Figure 5.

The PV module powers four (04) TE coolers (TEC1-12706) attached to the back of the absorber plate as shown in Figure 6. Fins, acting as heat sinks, were attached to the hot side of the TECs to enhance the heat transfer to the working fluid. The absorbing surface of the collector was 430 mm × 430 mm and the

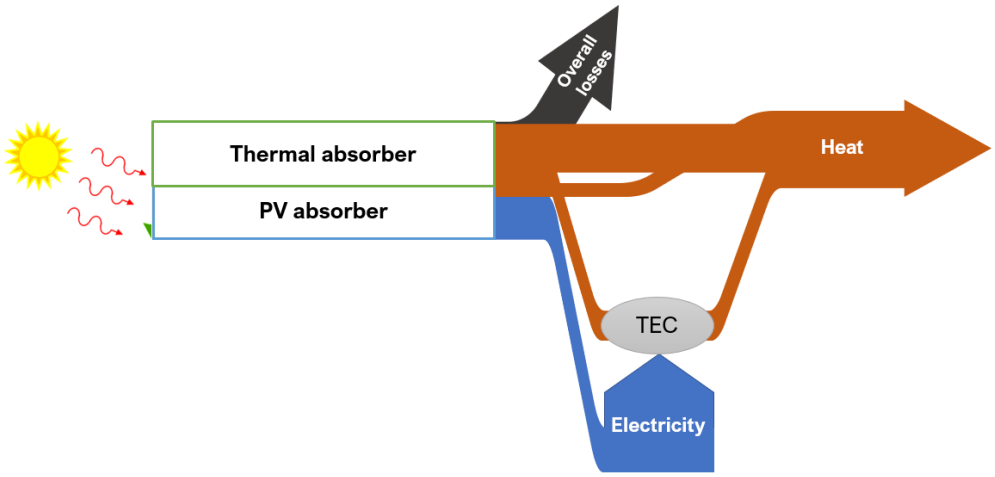

Figure 3. Energy balance in the TE heat pumping SAH

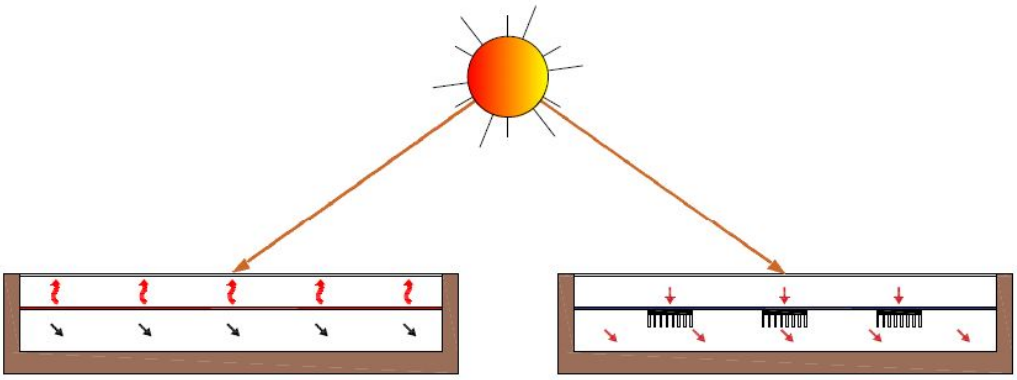

Figure 4. System description

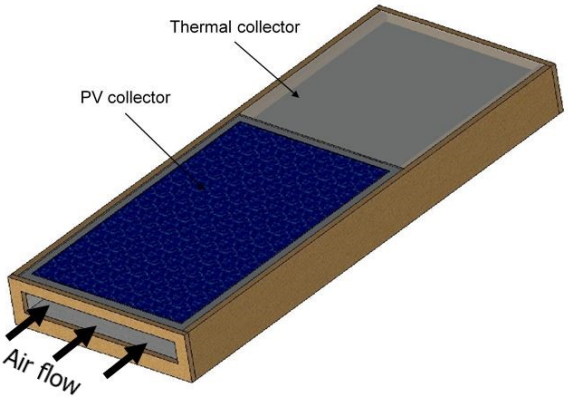

Figure 5. Overview design of the TE-heat pumping solar air heater

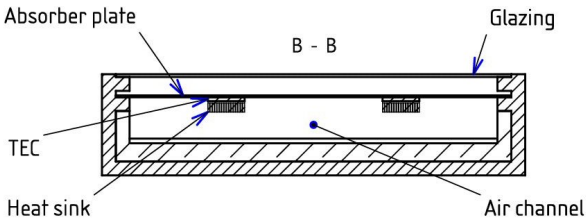

Figure 6. Cross-sectional view of the TE-heat pumping solar air heater

air channel was 430 mm × 45 mm. The airflow was designed to collect heat from both the PV module and the absorber plate while flowing beneath them, whereas the space between the absorber plate and the glazing was sealed to minimize thermal re-radiation from the absorber plate to the atmosphere. Table 1 presents the materials used for constructing the system. Table 2 presents the specifications of the TE modules and the PV module used. Figure 7 shows the arrangement of the TECs at the backside of the absorber plate. The cold sides of the TECs were in contact with the back surface of the absorber plate while heat sinks were attached to the hot sides of the TE module to increase the heat transfer to the working fluid (air).

2.2. Experimental methods

Two models of the system were constructed and tested in real conditions in Nsukka (6.8429°N, 7.3733°E), Nigeria. One was a conventional SAH with no TEC attached to the back of the absorber plate. This

Designation	Specifications
Glazing	A/R coated, 3 mm thick
Casing	Wood
Absorber plate	Al., 430 mm 430 mm, (Figure 7)
Insulation	Polystyrene, 25 mm thick
TE module	See Table 2
PV module	See Table 2

TABLE 1. Materials specifications for SAH construction

TE module	
Model	TEC1-12706
Couples N	127
Dimensions [mm]	40 × 40 × 4.2
ΔT_{max} [K]	68
$Q_{max}[W]$	63
Operating temperature T_{max} [°C]	138 °C
Operating current [A]	6 A max
Operating voltage [V]	14.4 V max
PV module	
Model	HU 40
Cell type	Mono-Si
P_{max}[W]	40 ±3 %
Cell efficiency [%]	17.3
Dimensions [mm]	670×430×22

TABLE 2. TE and PV modules specifications

prototype served as the control system for evaluating the performance of the second model with TE heat pumping. In this paper, the tests on the reference SAH will be referred to as Scenario A while the tests on the TE-SAH will be referred to as Scenario B. Natural air circulation through the collectors was adopted in this study. The electrical output of the PV module was connected to the TE modules which were connected in series of two to ensure that the maximum output voltage of the PV module was less than the maximum operating voltage of a single TEC. The electrical arrangement of the TECs is presented in Figure 8 and as such, the current and voltage input to each TE module was:

$$I_{in} = \frac{I_{out}}{2}, \tag{1}$$

$$V_{in} = \frac{V_{out}}{2}, \tag{2}$$

yielding the power input to each TEC as

$$P_{in} = \frac{I_{out}}{2}\frac{V_{out}}{2} = \frac{P_{out}}{4}. \tag{3}$$

This showed that the power input to the TECs could be improved by improving the PV energy output. This PV output could increase with better weather conditions or through the use of a PV module of a higher rating, supplying more power to the TECs, which would perform better and improve the performance of the system.

A data logging solarimeter (TES-1333R) was used to measure the insolation incident on the absorbing

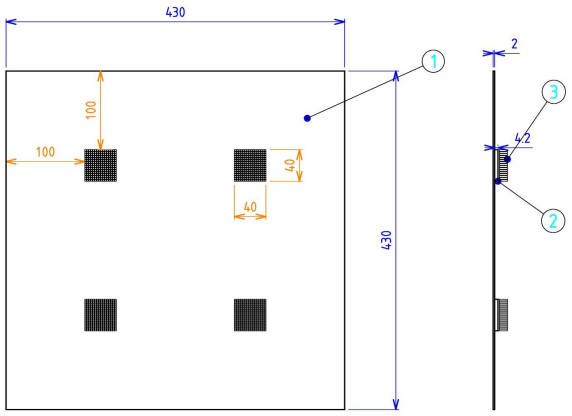

FIGURE 7. TECs arrangement on the absorber plate. 1. Absorber plate; 2. TE Cooler; 3. Heat sinks.

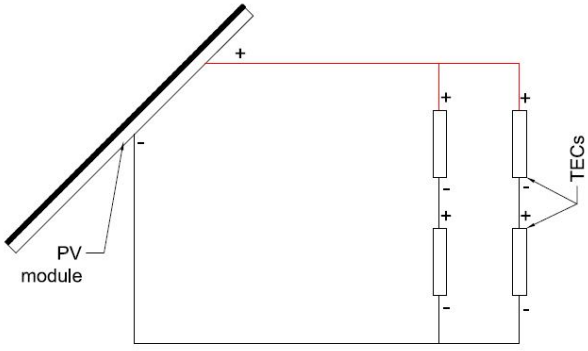

FIGURE 8. Electrical connection of the TECs

surface, a digital multimeter (UNI-T UT61 C) was used to measure the output voltage and current of the PV module, and a hot wire anemometer (BENETECH GM 8903) was used to measure the velocity of the air flowing through the collector. A multichannel temperature meter (APPLENT AT4208) was used to measure the temperature at different points (inlet, outlet, absorber plate, TE ends) of the SAH. The collector was tilted at an angle of 25° in the horizontal direction, determined by previous works in the same location [3, 34] as the optimal angle. The setup (presented in Figure 9) was monitored from 8:00 to 16:00 GMT and the data collected were analyzed to investigate the performance of the system. Due to the availability of only one set of measuring instruments, only one prototype with interchangeable absorber plates (one with TEC, and the other without) was constructed. Thus, the data collection was done on different days.

2.3. PERFORMANCE ANALYSIS

The collected data were analysed to evaluate the performance of the systems. The heat gain and the thermal energy efficiency were of interest in this study. The thermal energy production rate is computed as:

$$Q_u = \dot{m}c(T_{out} - T_{in}), \tag{4}$$

Figure 9. Experimental setup

$$\dot{m} = \rho v A_d, \tag{5}$$

where v is the air velocity $[\mathrm{m\,s^{-1}}]$, and A_d is the cross-sectional area of the collector $[\mathrm{m^2}]$. The power output of the PV module is determined as:

$$P_{out} = I_{out} V_{out}. \tag{6}$$

The instantaneous thermal energy efficiency relates the heat output to the energy input, and is obtained by:

$$\eta_{th} = \frac{Q_u}{S A_c}, \tag{7}$$

where S is the irradiance $[\mathrm{W\,m^{-2}}]$. Alternatively, the instantaneous efficiency of the solar air heater can be expressed as [35]:

$$\eta_{th} = F_R(\tau_e \alpha_c) - F_R U_L \frac{T_{av} - T_{amb}}{S}, \tag{8}$$

where α_c is the absorptance of the absorber plate ($\alpha_c = 0.85$ for black coated galvanised sheet, $\tau_e = 0.96$ for A/R coated glass used as glazing [36]), F_R is the heat removal factor, U_L is the heat loss factor, $T_{av} = \frac{T_{out}+T_{in}}{2}$ is the average temperature of the collector. From Equation 8, the heat removal factor can be calculated as

$$F_R = \frac{\eta_{th}}{\alpha_c \tau_e - U_L \frac{T_{av}-T_{amb}}{S}}. \tag{9}$$

The cumulative efficiency relates the cumulative heating rate to the cumulative energy input rate to the system and is computed using Equation 10 [37]

$$\eta_{cum} = \frac{\int_0^t \dot{m} c (T_{out} - T_{in}) \mathrm{dt}}{\int_0^t (S A_c) \mathrm{dt}}, \tag{10}$$

where Q_u is the air heating rate (W), $\dot{m}$ is the mass flow rate (kg/s) (Equation 5), c is the specific heat capacity of air $\left[\mathrm{JK^{-1}kg^{-1}}\right]$, T_{out} is the collector output temperature (K), and T_{in} is the inlet temperature [K]. ρ is the density of air $\left[\mathrm{kg\,m^{-3}}\right]$. As in the TE-SAH, the power output of the PV module is completely channeled into the TECs, as presented in Figure 3, only thermal energy output is obtained from this system. The overall losses of by the thermal collector Q_{loss} could be evaluated for estimation of the overall heat loss coefficient U_L (Equation 11).

$$U_L = \frac{Q_{loss}}{A_c(T_{av} - T_{amb})} = \frac{E_{in} - Q_u}{A_c(T_{av} - T_{amb})} \tag{11}$$

Figure 10 and Figure 11 present the variation of the irradiance and the air flow rate on the two days of data collection.

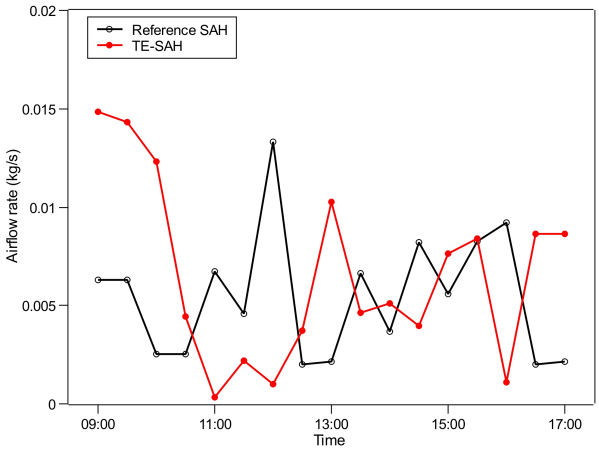

Figure 10. Test conditions: Airflow rate $\dot{m}$.

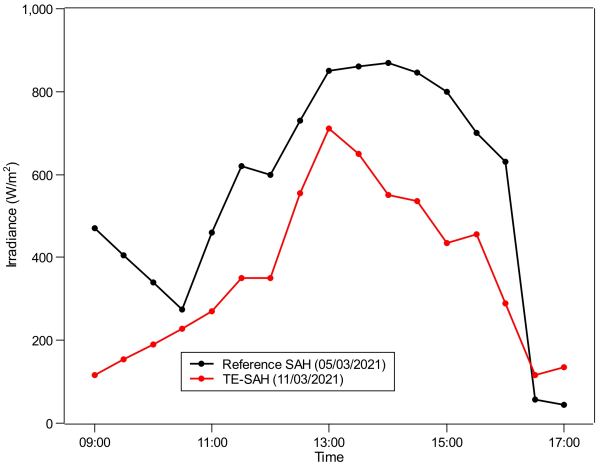

Figure 11. Test conditions: Irradiance S.

3. Results

The tests on the two systems were carried out on two different days at the same location and the parameters describing the performance were measured and analysed for the two systems. The irradiance not only varied from one day to the other, but also varied throughout each day, and this affected the operation of the collectors. The irradiance reached higher values for scenario A (with the reference SAH) than for scenario B (with the TE-SAH).

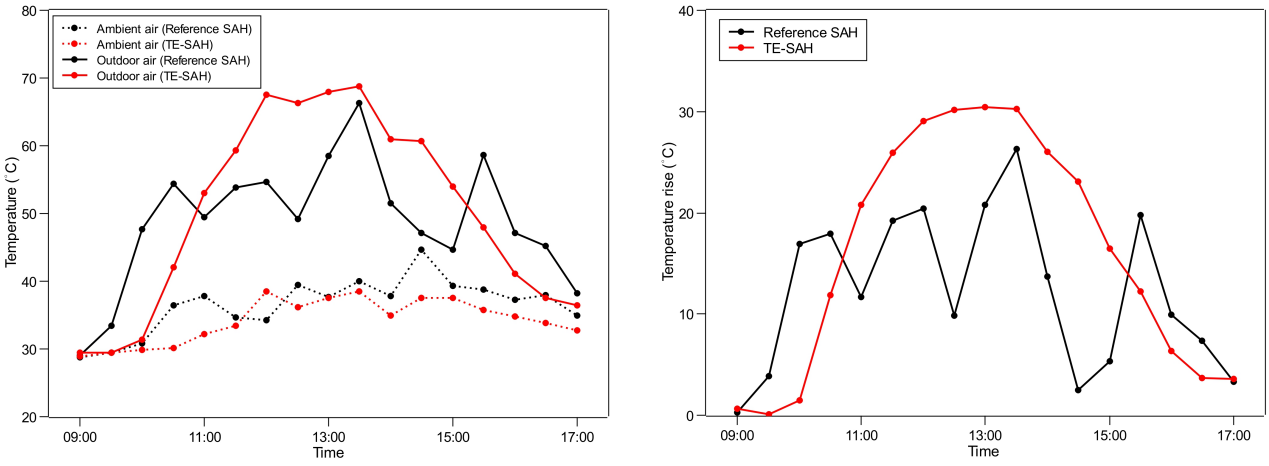

(A). T_{amb} and T_{out} (B). $T_{out} - T_{amb}$

FIGURE 12. Temperature variations for the SAH.

3.1. TEMPERATURE VARIATIONS

Figure 12a presents the temperature variations for the inlet (ambient) and outlet air temperature for both scenarios. Ambient air, at temperature T_{amb} varying between 28 °C and 39 °C, flowed by natural convection through the collector to remove heat from the absorbing surface (PV and thermal) and exited the collector with a higher temperature. The maximum T_{out} was 68.2 °C in the TE-SAH, higher than 64.3 °C measured in the reference SAH. The temperature rise (Figure 12b) followed the pattern of the variations of solar irradiance throughout the day. During the sun peak-hours (11:00–15:00), $T_{out} - T_{amb}$ were at their maximum. It can be seen from Figure 12b that the temperature rise was higher in the TE-SAH than in the reference SAH. The maximum $T_{out} - T_{amb}$ value in the TE-SAH was 32 °C, 6 °C higher than that achieved in the reference SAH (26 °C). The energy produced by the PV module powered the TECs at the back of the absorber plate, to pump heat from it. The heat was dissipated into the air duct by the fins attached to the TE hot side. Thus, the flowing air gained more useful heat, resulting in higher values of $T_{out} - T_{amb}$ for the TE-SAH than during the test on the reference SAH, and even though the incident irradiance was higher in the reference SAH than for the TE-SAH. After 15:00, when the solar irradiance started to decrease, the temperatures started to decrease too.

3.2. THERMAL ENERGY CONVERSION

The temperature rise, related to the air mass flow rate through the collector, was used to compute the thermal energy gain rate Q_u of the collector in the two scenarios Equation 4. Figure 13 presents the input and output energy of the two collectors. The input energy was higher for the reference SAH than for the TE-SAH, due to higher irradiance during the test with the reference SAH (Figure 13a). The heat gain varied for both scenarios throughout the day, being affected by the variations of the irradiance and the airflow rate (Figure 10 and 11). However Figure 13b shows that Q_u reached maximum values of 272.53 W at noon and 313.71 W at 13:00 for the reference SAH and the TE-SAH, respectively. After noon, the thermal energy gain was higher for the TE-SAH than for the reference SAH, depicting the additive effect of the TE heat pumping used in the TE-SAH. During the sun's peak hours, the electrical output, hence the power input to the TECs, increased. Thus, the TECs pumped more heat, adding to the heat collection by the air in the TE-SAH. Figure 14 presents the PV energy output for the two scenarios and the power input to a single TEC in the TE-SAH. The power output of the PV module was at its peak between 11:00 and 15:00, with a value ranging between 6 and 8 W.

Figure 15 shows that the cumulative heat gain Q_{cum} of the TE-SAH was lower than that of the reference SAH between 9:00 and 13:00, whereafter Q_{cum} values were higher for the TE-SAH than for the reference SAH. Thus, the TE-SAH had a higher thermal energy production rate than the reference SAH. The cumulative heat gain, for the duration of the experiment was 2.25 MJ for scenario B against 2.10 MJ for scenario A. Thus, the application of TE heat pumping contributed to a 7.14 % increase in the thermal energy production of the solar collector, despite the difference in the energy input.

Furthermore, the thermal energy losses were determined and compared for the two scenarios to evaluate the effect of TE heat pumping on the thermal losses of the air collector. Using Equation 11, the heat loss coefficient U_L was calculated for both the reference and TE-integrated collectors. The average value of U_L was 5.4 $\mathrm{W\,m^{-2}\,K^{-1}}$ and 3.4 $\mathrm{W\,m^{-2}\,K^{-1}}$ for the reference collector and the TE-integrated collector, respectively. Thus, the TE-SAH's heat loss coefficient was also reduced compared to the reference SAH. Hence, correspondingly, the thermal heat losses were reduced due to the application of TE-heat pumping.

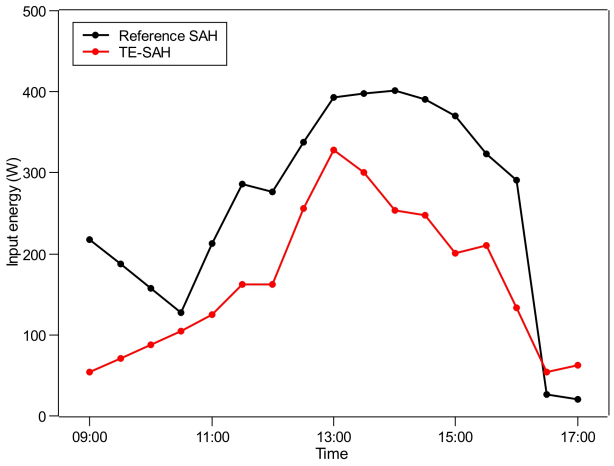

(A). Input energy E_{in}

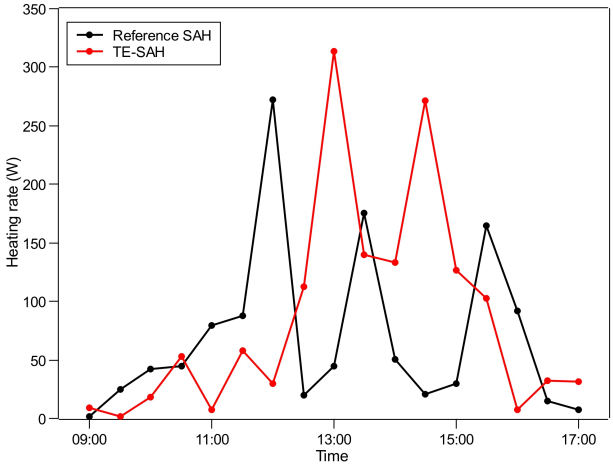

(B). Output energy Q_u

Figure 13. Energy flow for the SAH.

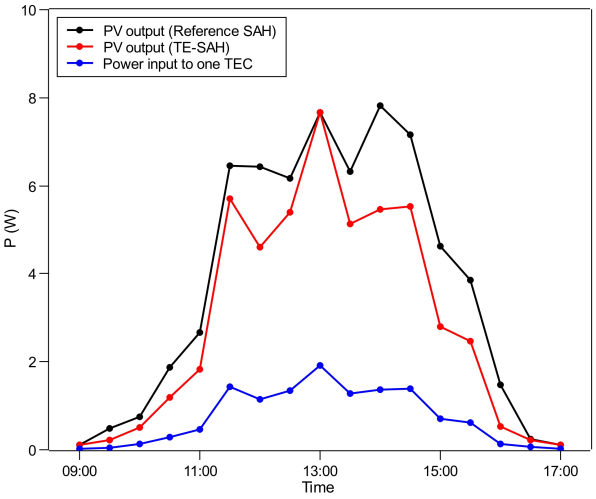

Figure 14. Output energy of the PV module and energy input to the TECs.

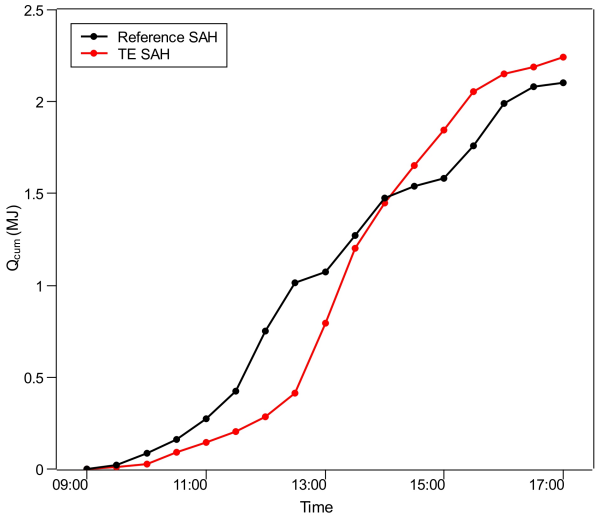

Figure 15. Cumulative thermal energy gain.

As shown in Figure 16a, the instantaneous values of heat loss Q_{loss} were higher for the reference SAH than for the TE-SAH, during peak sun hours when the PV electrical output was channeled into the TECs to perform heat pumping from the absorber plate, thus also increasing the heat collection by the working air. The maximum values of Q_{loss} were 55.1 W and 23.0 W for the reference SAH and TE-SAH, respectively. Figure 16b compares the cumulative thermal heat losses for the two collectors. It can be seen that the reference collector lost more thermal energy than the TE-SAH. Throughout the tests, the cumulative heat losses were evaluated at 0.39 MJ for the TE-SAH, and 0.85 MJ for the reference SAH. Thus, the thermal heat losses were reduced by 0.46 MJ, corresponding to a decrease of 54.12 %, due to the application of TE heat pumping. Also, as shown in Figure 17, the absorber plate temperatures for the TE-SAH reached lower values than for the reference SAH. This is the combined effect of the lower irradiance incident in the case of the TE-SAH, compared to the reference SAH, and the application of the TE heat pumping. Thus, with PV-TE heat pumping, the electricity from the PV module is used by the TEC to pump heat from the absorber plate, and cooling it. Consequently, the lower temperatures of the absorber plate represent an important driver of the reduced heat losses observed in Figure 16.

3.3. Thermal energy efficiency

Figure 18 compares the instantaneous energy efficiencies of the solar collectors in the two scenarios. The energy efficiency was significantly increased with the application of TE heat pumping. Between 12:00 and 15:00, due to maximum irradiance, the PV output was at its maximum (Figure 14), powering the TECs which pumped heat from the absorber plate, increasing the temperature at the TE hot side, thus allowing the working air to acquire more useful heat, which increased the thermal efficiency of the system. Figure 19 compares the cumulative efficiencies of the SAH in

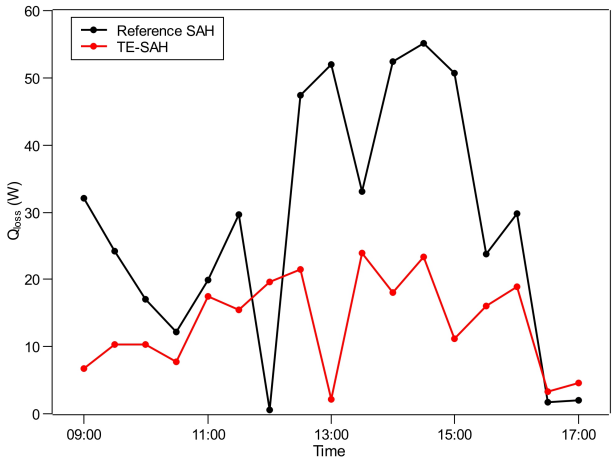

(A). Instantaneous

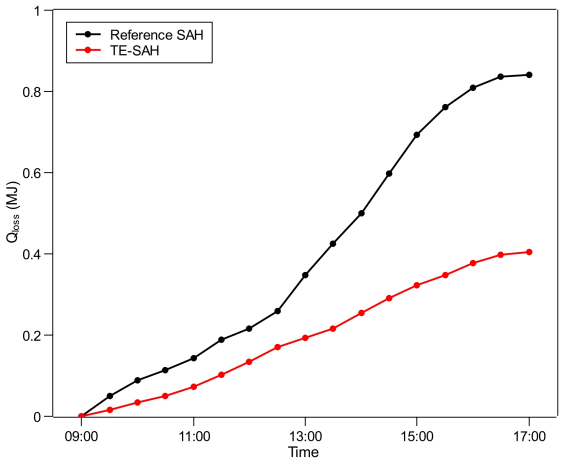

(B). Cumulative

FIGURE 16. Energy losses.

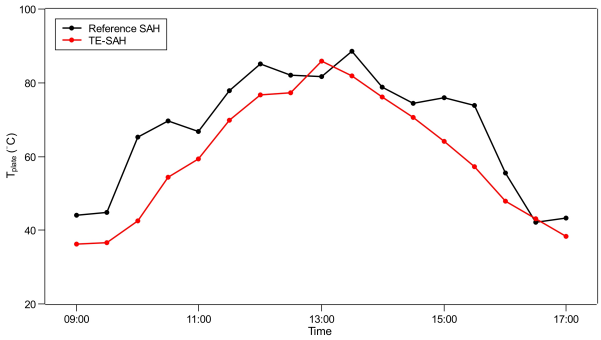

FIGURE 17. Absorber plate temperatures.

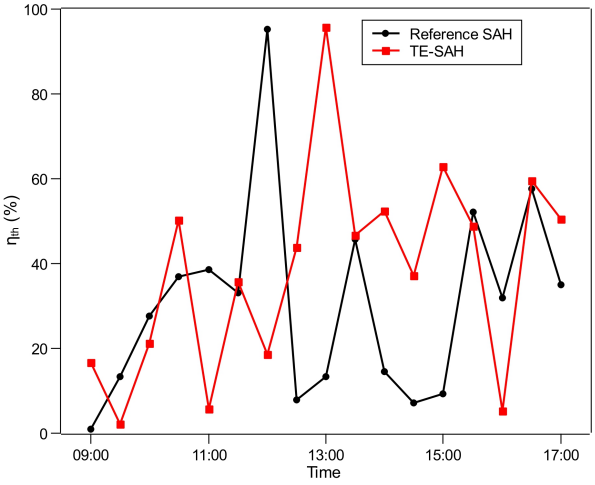

FIGURE 18. Energy efficiency.

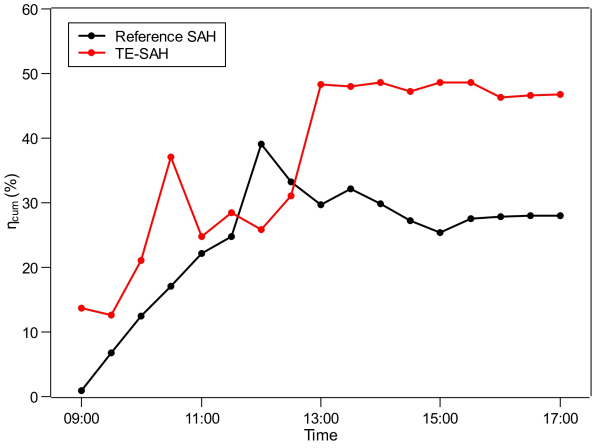

FIGURE 19. Cumulative energy efficiency.

the two scenarios, throughout the experiments. At the end of the day, the cumulative efficiencies of the SAH were 28.03 % and 46.73 % for scenarios A and B, respectively, representing an increase of 66.71 % in energy efficiency. This shows that TE heat pumping also increased the energy efficiency of the collector. Also, using Equation 8–9, the heat removal factor was also estimated and compared for the two collectors. The average value of F_R was 0.49 for the reference SAH, and 0.55 for the TE integrated SAH. Thus, with the application of TE heat pumping, the heat removal factor was also improved by 0.06, corresponding to an increase of 12.24 %.

4. CONCLUSIONS

In conclusion, the integration of thermoelectric coolers (TECs) as heat pumps into a solar air heater (SAH) demonstrated notable improvements in performance parameters in our outdoor setup. By using the output energy from a photovoltaic (PV) module to power the TECs attached to the SAH absorber plate, we observed a significant increase in the outlet air temperature compared to a reference SAH, despite lower irradiance intensity.

Specifically, the temperature rise in the TE heat pumping SAH surpassed that of the reference SAH.

Notably, although the input energy was lower for the TE-SAH, the energy output was improved, particularly during peak sunlight hours when the PV electrical output reached its maximum, enabling effective heat pumping by the TECs. As a result, the TE heat pumping system improved heat collection by 7.14 %.

Furthermore, the energy efficiency of the TE heat pumping SAH reached 46.73 %, which is 66.73 % higher than the conventional SAH with an energy efficiency of 28.03 %. This improvement was accompanied by a reduction in heat loss coefficient and overall heat losses, leading to a decrease in heat losses by 0.46 MJ over the test duration. Additionally, the heat removal factor F_R experienced an increase with the incorporation of TE heat pumping.

It is crucial to note that the performance of the TE heat pumping system is intricately tied to the power input to the TECs, directly dependent on the PV electrical energy output. This study demonstrates the effectiveness of utilising TECs as heat pumps in solar air heaters, offering a more efficient and environmentally sustainable approach to improve heat collection and energy efficiency in solar thermal systems.

List of symbols

A_c Collector absorbing surface area [m^2]
A_d Collector cross- sectional surface area [m^2]
c Specific heat capacity [$J/K\,kg^{-1}$]
I Current [A]
P Power, Heat removal rate [W]
S irradiance [$W\,m^{-2}$]
T Temperature [K]
v Air velocity [$m\,s^{-1}$]
η Efficiency [%]
ρ Air density [$kg\,m^{-3}$]

Acknowledgements

The authors of this paper would like to thank the German Academic Exchange Service (DAAD) which funded this research through the In-Region scholarship programme. Additional funding for this research was provided by the Association of Commonwealth Universities (ACU) Engineering (Wighton) Fellowship.

References

[1] IRENA. Renewable capacity statistics 2019. Tech. rep., International Renewable Energy Agency, 2020. [2021-03-03]. https://www.irena.org/Publications

[2] A. A. El-Sebaii, S. M. Shalaby. Solar drying of agricultural products: A review. *Renewable and Sustainable Energy Reviews* **16**(1):37–43, 2012. https://doi.org/10.1016/j.rser.2011.07.134

[3] S. O. Enibe. Performance of a natural circulation solar air heating system with phase change material energy storage. *Renewable Energy* **27**(1):69–86, 2002. https://doi.org/10.1016/S0960-1481(01)00173-2

[4] D. Zenhäusern, E. Bamberger, A. Baggenstos, A. Häberle. PVT Wrap-Up: Energy systems with photovoltaic-thermal solar collectors. Technical report, 2017.

[5] S. Diwania, S. Agrawal, A. S. Siddiqui, S. Singh. Photovoltaic–thermal (PV/T) technology: a comprehensive review on applications and its advancement. *International Journal of Energy and Environmental Engineering* **11**(1):33–54, 2020. https://doi.org/10.1007/s40095-019-00327-y

[6] A. Al-Waeli, K. Sopian, H. A. Kazem, M. Chaichan. Photovoltaic solar thermal (PV/T) collectors past, present and future: A review. *International Journal of Applied Engineering Research* **11**(22):10757–10765, 2016. https://doi.org/10.5281/zenodo.8040609

[7] A. Fudholi, M. Zohri, I. Taslim, et al. Heat transfer and efficiency of dual channel PVT air collector: a review. *International Journal of Power Electronics and Drive Systems* **10**(4):2037–2045, 2019. https://doi.org/10.11591/ijpeds.v10.i4.pp2037-2045

[8] A. Z. Sahin, K. G. Ismaila, B. S. Yilbas, A. Al-Sharafi. A review on the performance of photovoltaic/thermoelectric hybrid generators. *International Journal of Energy Research* **44**(5):3365–3394, 2020. https://doi.org/10.1002/er.5139

[9] S. Thongsan, B. Prasit, T. Suriwrong, et al. Development of solar collector combined with thermoelectric module for solar drying technology. *Energy Procedia* **138**:1196–1201, 2017. https://doi.org/10.1016/j.egypro.2017.10.388

[10] N. Dimri, A. Tiwari, G. N. Tiwari. Comparative study of photovoltaic thermal (PVT) integrated thermoelectric cooler (TEC) fluid collectors. *Renewable Energy* **134**:343–356, 2019. https://doi.org/10.1016/j.renene.2018.10.105

[11] N. S. Nazri, A. Fudholi, M. H. Ruslan, K. Sopian. Mathematical modeling of photovoltaic thermal-thermoelectric (PVT-TE) air collector. *International Journal of Power Electronics and Drive Systems* **9**(2):795–802, 2018. https://doi.org/10.11591/ijpeds.v9.i2.pp795-802

[12] C. Babu, P. Ponnambalam. The role of thermoelectric generators in the hybrid PVT systems: A review. *Energy conversion and Management* **151**:368–385, 2017. https://doi.org/10.1016/j.enconman.2017.08.060

[13] F. Masood, N. B. M. Nor, P. Nallagownden, et al. A review of recent developments and applications of compound parabolic concentrator-based hybrid solar photovoltaic/thermal collectors. *Sustainability* **14**(9):5529, 2022. https://doi.org/10.3390/su14095529

[14] F. Masood, N. B. M. Nor, I. Elamvazuthi, et al. The compound parabolic concentrators for solar photovoltaic applications: Opportunities and challenges. *Energy Reports* **8**:13558–13584, 2022. https://doi.org/10.1016/j.egyr.2022.10.018

[15] K. S. Ong. Review of solar, heat pipe and thermoelectric hybrid systems for power generation and heating. *International Journal of Low-Carbon Technologies* **11**(4):460–465, 2016. https://doi.org/10.1093/ijlct/ctv022

[16] W.-Y. Chen, X.-L. Shi, J. Zou, Z.-G. Chen. Thermoelectric coolers: progress, challenges, and opportunities. *Small Methods* **6**(2):2101235, 2022. https://doi.org/10.1002/smtd.202101235

[17] D. Singh, H. Chaubey, Y. Parvez, et al. Performance improvement of solar PV module through hybrid cooling system with thermoelectric coolers and phase change material. *Solar Energy* **241**:538–552, 2022. https://doi.org/10.1016/j.solener.2022.06.028

[18] Y. Luo, L. Zhang, Z. Liu, et al. Performance analysis of a self-adaptive building integrated photovoltaic thermoelectric wall system in hot summer and cold winter zone of China. *Energy* **140**:584–600, 2017. https://doi.org/10.1016/j.energy.2017.09.015

[19] C. Wang, C. Calderón, Y. Wang. An experimental study of a thermoelectric heat exchange module for domestic space heating. *Energy and Buildings* **145**:1–21, 2017. https://doi.org/10.1016/j.enbuild.2017.03.050

[20] R. S. Kumar, N. P. Priyadharshini, E. Natarajan. Experimental and numerical analysis of photovoltaic solar panel using thermoelectric cooling. *Indian Journal of Science and Technology* **8**(36):252–256, 2015. https://doi.org/10.17485/ijst/2015/v8i36/87646

[21] D. Enescu, F. Spertino. Applications of hybrid photovoltaic modules with thermoelectric cooling. *Energy Procedia* **111**:904–913, 2017. https://doi.org/10.1016/j.egypro.2017.03.253

[22] X. Ma, G. Li. Building integrated thermoelectric air conditioners—a potentially fully environmentally friendly solution in building services. *Future Cities and Environment* **5**(1), 2020. https://doi.org/10.5334/fce.76

[23] V. P. Joshi, V. S. Joshi, H. A. Kothari, et al. Experimental investigations on a portable fresh water generator using a thermoelectric cooler. *Energy Procedia* **109**:161–166, 2017. https://doi.org/10.1016/j.egypro.2017.03.085

[24] L. Yang, Z.-G. Chen, J. Zou. High-performance thermoelectric materials for solar energy application. In *Emerging Materials for Energy Conversion and Storage*, pp. 3–38. Elsevier, 2018. https://doi.org/10.1016/B978-0-12-813794-9.00001-6

[25] A. Allouhi, A. Boharb, T. Ratlamwala, et al. Dynamic analysis of a thermoelectric heating system for space heating in a continuous-occupancy office room. *Applied Thermal Engineering* **113**:150–159, 2017. https://doi.org/10.1016/j.applthermaleng.2016.11.001

[26] Y. Cai, D.-D. Zhang, D. Liu, et al. Air source thermoelectric heat pump for simultaneous cold air delivery and hot water supply: Full modeling and performance evaluation. *Renewable Energy* **130**:968–981, 2019. https://doi.org/10.1016/j.renene.2018.07.007

[27] A. Fudholi, K. Sopian. Review on exergy and energy analysis of solar air heater. *International Journal of Power Electronics and Drive Systems* **9**(1):420–426, 2018. https://doi.org/10.11591/ijpeds.v9n1.pp420-426

[28] A. Fudholi, K. Sopian. A review of solar air flat plate collector for drying application. *Renewable and Sustainable Energy Reviews* **102**:333–345, 2019. https://doi.org/10.1016/j.rser.2018.12.032

[29] C. Mund, S. K. Rathore, R. K. Sahoo. A review of solar air collectors about various modifications for performance enhancement. *Solar Energy* **228**:140–167, 2021. https://doi.org/10.1016/j.solener.2021.08.040

[30] A. G. Lupu, V. M. Homutescu, D. T. Balanescu, A. Popescu. A review of solar photovoltaic systems cooling technologies. *IOP Conference Series: Materials Science and Engineering* **444**(8):082016, 2018. https://doi.org/10.1088/1757-899X/444/8/082016

[31] J. Siecker, K. Kusakana, B. P. Numbi. A review of solar photovoltaic systems cooling technologies. *Renewable and Sustainable Energy Reviews* **79**:192–203, 2017. https://doi.org/10.1016/j.rser.2017.05.053

[32] V. Oner, M. Yesilyurt, E. C. Yilmaz, G. Omeroglu. Photovoltaic thermal (PVT) solar panels. *International Journal of New Technology and Research* **2**(12):13–16, 2016.

[33] M. Seyednezhad, H. Najafi. Solar-powered thermoelectric-based cooling and heating system for building applications: A parametric study. *Energies* **14**(17):5573, 2021. https://doi.org/10.3390/en14175573

[34] C. Mgbemene, I. Jacobs, C. O. Agbo, et al. Experimental investigation on the performance of a solar air heater with the absorber plate made of aluminium soda cans. In *Nigeria beyond Recession: Unlocking the Potentials of Solar Energy for Economic Recovery*, pp. 1–13. Solar Energy Society of Nigeria Abuja, 2017.

[35] J. A. Duffie, W. A. Beckman. *Solar engineering of thermal processes*. Wiley, New York, 1991.

[36] The engineering toolbox: Solar radiation absorbed by various materials, 2009. [2021-03-12]. https://www.engineeringtoolbox.com/solar-radiation-absorbed-materials-d-1568.html

[37] J. A. Duffie, W. A. Beckman, N. Blair. *Solar Engineering of Thermal Processes, Photovoltaics and Wind*. John Wiley & Sons, 5th edn., 2020.